

hEARt: Motion-resilient Heart Rate Monitoring with In-ear Microphones

Kayla-Jade Butkow
University of Cambridge
United Kingdom
kjb85@cam.ac.uk

Ting Dang
University of Cambridge
United Kingdom
td464@cam.ac.uk

Andrea Ferlini
University of Cambridge
United Kingdom
af679@cam.ac.uk

Dong Ma
Singapore Management University
Singapore
dongma@smu.edu.sg

Cecilia Mascolo
University of Cambridge
United Kingdom
cm542@cam.ac.uk

ABSTRACT

With the soaring adoption of in-ear wearables, the research community has started investigating suitable in-ear heart rate (HR) detection systems. HR is a key physiological marker of cardiovascular health and physical fitness. Continuous and reliable HR monitoring with wearable devices has therefore gained increasing attention in recent years. Existing HR detection systems in wearables mainly rely on photoplethysmography (PPG) sensors, however, these are notorious for poor performance in the presence of human motion. In this work, leveraging the occlusion effect that can enhance low-frequency bone-conducted sounds in the ear canal, we investigate for the first time *in-ear audio-based motion-resilient* HR monitoring. We first collected the HR-induced sound in the ear canal leveraging an in-ear microphone under stationary and three different activities (i.e., walking, running, and speaking). Then, we devised a novel deep learning based motion artefact (MA) mitigation framework to denoise the in-ear audio signals, followed by an HR estimation algorithm to extract HR. With data collected from 20 subjects over four activities, we demonstrate that hEARt, our end-to-end approach, achieves a mean absolute error (MAE) of 4.51 ± 6.01 BPM, 9.95 ± 7.62 BPM, 13.57 ± 10.51 BPM and 11.71 ± 8.59 BPM for stationary, walking, running and speaking, respectively, opening the door to a new non-invasive and affordable HR monitoring with usable performance for daily activities. Not only does hEARt outperform previous in-ear HR monitoring work, but is comparable (and even better whenever full-body motion is concerned) to reported in-ear PPG performance.

1 INTRODUCTION

Heart rate (HR) is considered an excellent indicator of fitness level, strongly associated with cardiovascular disease and mortality risk. HR monitoring can help design workout routines to maximize training effect, and, more importantly, serves as an early biomarker for heart disease since cardiovascular fitness is one of the key predictors of cardiovascular disease. Additionally, heart rate variability (HRV), the change in time between successive beats, is a key predictor of physical and mental health. HRV is a proxy for autonomic nervous system behaviour, and is believed to be predictive of aerobic fitness when measured during both maximal and sub-maximal exercise [35]. Electrocardiographic (ECG) telemetry monitoring has been recognized as the standard approach for HR and HRV monitoring, however ECGs need to be connected to the body (with leads)

and are, therefore, unsuitable for use in realistic and mobile settings. Recent trends in wearables have led to a proliferation of studies that investigate different sensors on smartwatches, earables, and other wearables for HR monitoring, where photoplethysmography (PPG) sensors are most commonly adopted due to their non-invasiveness and practical measurement. Specifically, PPGs shine light onto the skin and measure the amount of light scattered by blood flow, which changes due to heart beats.

Although PPG is found to be effective and accurate for HR measurements under stationary conditions [7], it is sensitive to motion artefacts (MA) caused by user's body movement or physical activities [1, 7, 23, 25, 37, 50]. This motion noise usually manifests itself with large amplitude in the PPG signal and overlaps with the heart rate signal in the frequency domain [21]. This is commonly tackled by using a reference signal from accelerometers for motion estimation and then by removing this signal from the PPG measurements [10]. However, to do this, an additional sensor is required, and the accuracy still does not match that of the stationary case [7]. Dealing with interference from motion artefacts is generally an open and challenging problem in HR estimation research.

Current earables are equipped with many sensors, including outer and inner ear microphones which fulfil fundamental functionalities of the device (e.g., speech detection and active noise cancellation). Recently, Martin and Voix [32] proposed to measure HR using a microphone placed in the human ear canal. When the ear canal opening is sealed by the earbuds, the cavity formed between the ear tip and eardrum enables an enhancement of low-frequency sounds, called the occlusion effect [44]. As a result, heartbeat-induced sounds that propagate to the ear canal through bone conduction are amplified and can be leveraged for HR estimation. Moreover, due to the rapid spreading of ear-worn wearables (earables) in daily life [24], earables can be a portable and non-invasive way for continuous HR detection under various scenarios. However, [32] only demonstrated the feasibility of measuring HR with in-ear microphones while an individual is stationary: *how in-ear microphone HR measurement performs under active scenarios remains unclear and unexplored*.

In this work, we focus on in-ear HR estimation under both stationary and active scenarios (e.g., walking, running and speaking). The biggest hurdle to accurate HR measurement is the motion-induced interference, originating from the fact that the occlusion effect amplifies not just the heartbeat-induced sounds, but also

the sounds/vibrations generated by these activities [31]. Removing such interference is non-trivial and poses three challenges. First, as the strength of heartbeats is much weaker than the foot strikes, heartbeat signals are buried in the walking signals. Second, since HR and walking frequency (i.e. cadence) are quite similar (both around 1.5-2.3Hz [36]), it is hard to separate them in the frequency domain. Third, due to the proximity of the ear to the human vocal system, human speech and its associated jaw movements can overwhelm the heartbeat-induced sound.

To address these challenges, we propose a processing pipeline for accurate HR detection in the presence of motion artefacts, namely, walking, running and speaking. Specifically, (1) based on the challenges in separating heart and activity sounds, we develop a convolutional neural network (CNN) to clean heart sounds with the supervision of ground truth (GT) ECG signals. ECG signals are only required during model training, but are not needed for test or deployment. We further leverage transfer learning that pre-trains the denoising CNN using a large heart sound database (PASCAL) and fine-tunes it using our data, to account for the small data set. (2) using the resultant cleaned signals, we compute the HR using a simple signal processing pipeline. (3) differently from previous audio-based HR estimation works [19, 32, 39, 40], we additionally validate the functioning of our technique in the presence of human speech, showing how the proposed approach can successfully deal with speaking activities.

With data collected from 20 subjects, we demonstrate that an in-ear microphone can be a viable sensor for HR estimation under motions with good performance. As a coarse comparison, such performance is even superior to most of the PPG-based approaches as reported in the literature [7, 16, 50]. Specifically, because of the considered artifacts, the vantage points (the ears), and the device form-factor (earables) used, our work is directly comparable to [16]. Notably, we significantly outperform our PPG counterpart for both walking and running achieving a mean absolute percentage error of 14.08% and 12.75%. This is 27.14% and 29.84% better than in-ear PPG for walking and running respectively [16]. This is a remarkable result hinting at the great potential of in-ear microphone for cardiovascular health monitoring, even under challenging situations. Moreover, compared to a PPG sensor, the microphone is more energy efficient [26, 34] and affordable, offering additional appeal for continuous HR estimation.

The contribution of this work can be summarized as:

- We explore HR estimation with in-ear microphones and present an exhaustive analysis of the interference imposed by common human activities.
- We propose a novel pipeline for HR estimation under motion artefacts. It consists of a CNN-based module using U-Net architecture to enhance audio-based heart sounds with ECG as a reference, and an estimation module using signal processing techniques to estimate HR from clean heart signal. We further leverage transfer learning that pre-trains the model using a large heart sound database and fine-tunes it using our data, to effectively capture heart sounds related information as well as handling the limited data size. To the best of our knowledge, no previous works have attempted to clean

and enhance audio-based heart sounds captured by earables using ECG signal.

- We build an earbud prototype with very good signal-to-noise ratio (SNR). We collected data from 20 subjects, which we will release to the research community.
- Our results show that we can achieve mean absolute errors of 4.51 ± 6.01 BPM, 9.95 ± 7.62 BPM, 13.57 ± 10.51 BPM and 11.71 ± 8.59 BPM for stationary, walking, running and speaking, respectively, demonstrating the effectiveness of the proposed approach on combating the motion artefacts. This performance is comparable (and even better whenever full-body motion is concerned) to in-ear PPG performance in literature.

2 PRIMER

In this section, we first motivate our work by providing a brief evolution of different HR detection techniques, including the preliminary research into in-ear microphone based HR detection in a static setting. We then present the challenges of achieving accurate and portable in-ear HR estimation in more realistic conditions.

2.1 Motivation

ECG is one of the most common methods for HR measurement and it is often regarded as the golden standard. However, it is not very portable and requires leads connected to various parts of the body to be accurate. Although attempts to devise portable ECG, such as ECG chest straps, have been introduced, they remain cumbersome, uncomfortable, and inconvenient for every day use, leading to a low social acceptance. Some new smartwatches contain a single-lead ECG, however they require the user to remain still and to close the ECG circuit with their fingers. They are thus unable to perform continuous monitoring.

On the other hand, in the last 5-10 years, PPG sensors have been widely adopted for continuous HR monitoring with wearable devices, due to their non-intrusive, relatively simple and inexpensive measurements. However, as of today, the research community has yet to find an agreement on the goodness of wrist-worn PPG (e.g. PPG on smartwatch). While the topic has been widely investigated [1, 7, 9, 37], a consensus on the best commercially available device to monitor the wearer’s HR, whenever motion is concerned, is yet to be found. Moreover, intense motion, like walking and running, yields substantial deviations from GT, resulting in average errors up to 30% across a wide-spectrum of wrist-worn devices [7]. Other factors may come into play as well: for instance, the fit of the watch is key to achieve acceptable HR measurements. A more comfortable/loose fit of the smartwatch correlates with drastic performance degradation [1]; skin perfusion and the presence of tattoos are reported to be a deterrent to accurate HR monitoring [7].

Due to the limitations of wrist-based PPG, researchers have started looking into earables (ear-worn wearables) as an alternative (or companion) to smartwatches for continuous HR sensing [19]. While today this is mostly a research vision, Jabra has recently launched the Jabra Elite Sport¹, a pair of earbuds equipped with a Valencell² PPG sensor to measure HR from the user’s concha (i.e.

¹<https://www.jabra.com/sports-headphones/jabra-elite-sport>

²<https://valencell.com/>

the depression of the outer ear in the proximity of the ear-canal). However, despite being a fascinating and promising device, their real world performance under motion is still relatively poor [16, 37]. Indeed, similarly to what is observed for wrist-worn devices [7], errors around 30% have been reported for earables [16].

Like with in-ear PPG sensing, in-ear audio sensing for HR monitoring is also a recent area of research, with very scarce literature. Recent work [32] has proposed in-ear audio using a microphone for HR and respiratory rate measurements. Their results show a MAE of 4.3 BPM and a mean difference estimate of -0.44 BPM with a limit of agreement (LoA) interval of -14.3 to 13.4 BPM. This points at the potential of in-ear audio-based HR monitoring. However, the work only investigates the stationary setting, and a higher error is reported for the time period when the subject’s body is in motion. Motivated by these findings, we aim to explore the power of in-ear audio sensors for accurate HR detection under typical daily motion conditions including walking, running, and speaking.

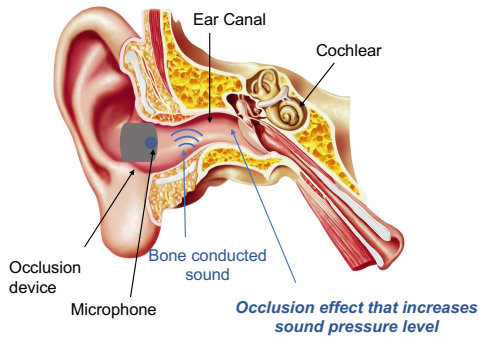


Figure 1: Illustration of the occlusion effect and the anatomy of the ear.

2.2 In-ear Heart Sound Acquisition

We now describe the mechanism by which heart sounds are generated and captured inside the ear canal. Bone conduction, a physiological phenomenon whereby sound is conducted through the bones directly to the inner ear, causes vibrations in the walls of the ear [44]. When the ear canal is occluded, there is an increase in impedance at the entrance to the ear canal, which results in an amplification of the low frequency sounds conducted by the bones [44]. This effect, which is illustrated in Figure 1, is known as the occlusion effect. Since bone generally conveys low-frequency sounds [47], the bone-conducted heart sounds will be amplified in the occluded ear canal [32]. Heart sounds can thus be detected using a microphone placed inside the occluded ear canal. An example showing the heart sounds captured by the internal microphone is shown in Figure 2. It is evident that the two sounds in the cardiac cycle (S1 and S2) can be captured using the in-ear microphone, thus indicating the potential of in-ear microphones to be used for HR monitoring. The correlation between the in-ear captured audio and the ECG signal is also evident in Figure 2. Here, the QRS complex (the combination of three of the graphical deflections seen on a

typical electrocardiogram³) of the ECG, as shown in Figure 2, which occurs due to ventricular depolarization [48], corresponds to the S1 heart sound. The T and P waves seen in Figure 2 occur due to ventricular repolarization and atrial depolarization respectively. The end of the ECG T wave corresponds to the S2 heart sound [48].

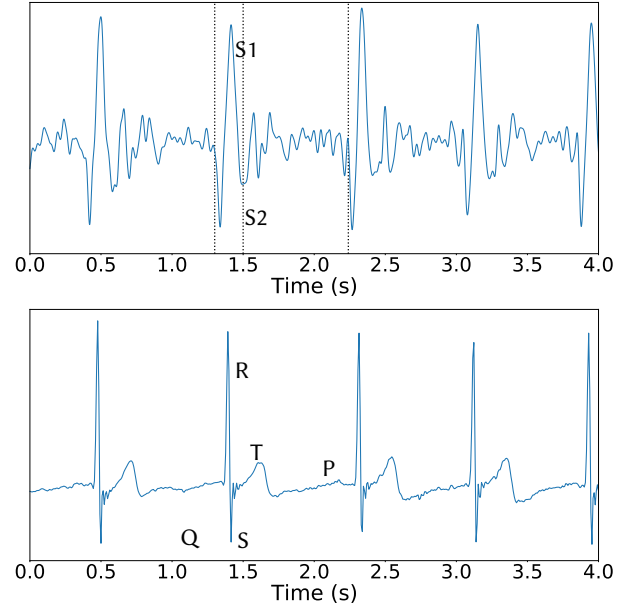


Figure 2: The (left) sound signal captured by the internal microphone for one window and the (right) ECG signal for the corresponding window for the same participant.

2.3 Motion Artefacts Analysis and Challenges

In-ear microphone based HR estimation suffers from human motion artefacts since the occlusion effect not only amplifies the heartbeat-induced sound, but also enhances other bone-conducted sounds and vibrations inside the body [15, 31]. Figures 3a to 3d illustrates the recorded audio signals from the in-ear microphone while stationary, walking, running and speaking, and Figures 3e to 3h are their corresponding spectrograms. The heartbeat is clearly observable when an individual is stationary in Figure 3a, with frequency lying around 1.2Hz and its 1st and 2nd harmonics clearly observable in Figure 3e. Contrastingly, it is completely overwhelmed by the amplified step sounds in Figure 3b (note the different scales of the y-axis), with the periodic peaks corresponding to the sound of foot strikes that propagates through the human skeleton, with a significantly higher energy observed around 1.7Hz in Figure 3f. Though the heart sound frequency and its harmonics are still observable, it is difficult to estimate HR directly from the raw corrupted audio signals. Furthermore, it is evident that the periods of heart sounds and walking are similar, resulting in an overlap in the frequency domain, which makes it challenging to split the heart sounds and walking signals and estimate the HR either in time domain or frequency domain.

³https://en.wikipedia.org/wiki/QRS_complex

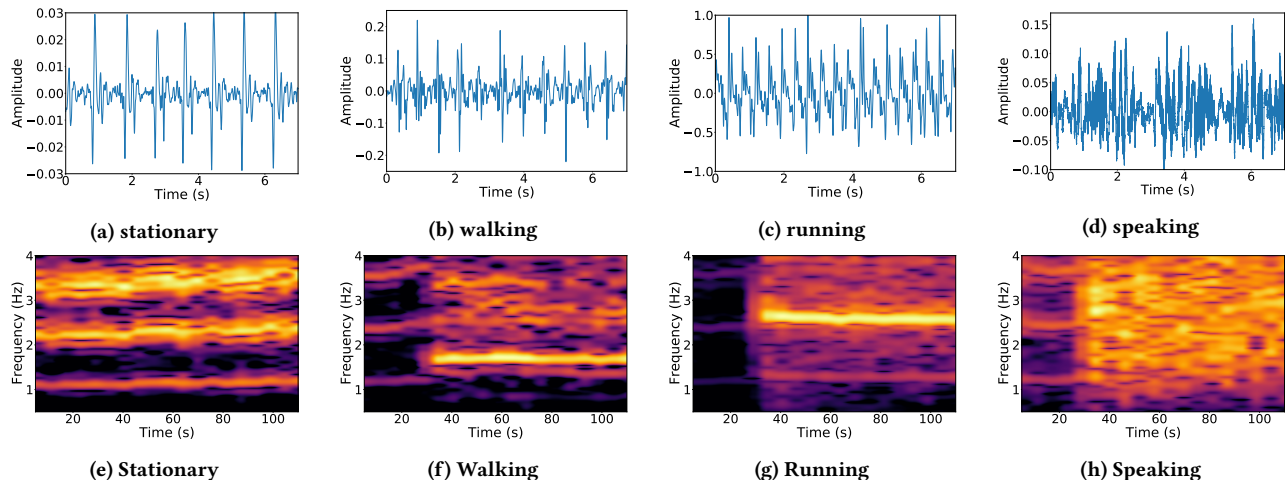


Figure 3: Time domain representations and spectrograms of the audio signals captured by the in-ear microphone over the four activities.

The heartbeats are further affected by foot strikes during running that exhibits far stronger energy than any of the other activities in Figure 3c, with high energy in 2.6Hz in Figure 3g corresponding to the frequency of the foot. The speech sound in Figure 3d also shows strong amplitudes due to the proximity of the ear and human vocal system, making the heartbeat-induced sound indiscernible. As in Figure 3f, the frequency components span over 1Hz to 4Hz and mask the heart sounds, due to the jaw movement during speaking that creates some vibrations and obscures the heart signals [6].

Next, we present our approach to overcome these challenges.

3 MOTION-RESILIENT HR ESTIMATION

Typical signal processing techniques have shown effectiveness in HR estimation in the user stationary case [32]: we adopt these approaches in this case also due to their low computational costs. However, they do not adequately isolate the heart sounds from the corrupted audio under motion artefacts. As previously discussed, motion-artefact elimination is a non-trivial problem. Typical signal processing techniques for denoising are more effective under certain signal-to-noise ratios (SNR) and errors increase with decreased SNR [2, 3]. Additionally, the differences in the user’s anatomy (different ear canal shapes, different earbud fit levels and thus changes in the resultant amplification) result in differences in the captured audio sounds, and this variability may not be well captured and processed using signal processing techniques. Due to the recent successes witnessed by deep learning (DL) for denoising in a variety of fields [18, 30], we propose a novel pipeline using deep learning to eliminate motion artefacts in audio signals and further estimate HR.

When capturing audio inside the ear canal, heart sounds cannot be recorded during motion without simultaneously collecting motion artefacts. This makes denoising of heart sounds difficult as clean ground truth heart sounds cannot be captured during motion. Similar to PPG-based denoising approaches [46], we recorded ECG data simultaneously during the audio data collection, and use ECG as a reference signal providing a relative clean and high-quality

heart signal under motion artefacts. We developed neural networks to map the noisy heart sound signal to its corresponding ECG (a clean heart signal), and further estimated HR from the output *synthesized ECG*. Our problem is thus framed as a denoising problem but also as a synthesis problem. After the neural network is properly trained, we can directly employ it to obtain the clean heart signal for HR estimation. Therefore, ECG is only required for model training, but not for testing nor during real deployment of the technique.

In the following sections, we first present a signal processing approach for HR estimation for stationary case, and then the proposed DL pipeline for motion artefacts removal.

3.1 Signal Processing for HR Estimation

As shown by Martin and Voix [32], it is possible to obtain high accuracy for HR determination using in-ear audio while stationary. As such, the initial phase of our work involved the development of a signal processing pipeline for HR estimation. This aims to provide an efficient and computationally effective HR detection method for the stationary case, and also to explore the potential of typical signal processing techniques in HR estimation under motion artefacts. Different from [32] which uses a peak detection technique on the pre-processed waveform, we detect HR from the frequency domain.

First, we compute the Hilbert transform of the audio signals to calculate the HR envelope. We then compute the spectrum of the envelope using Fast Fourier Transform (FFT) and detect the dominant peaks which are converted to the HR. This approach shows good performance on a clean and stationary signal (as shown in Section 5.2). However, when audio signals are corrupted with motions, dominant peaks in the spectrum may correspond to motions, rather than the HR, thus introducing errors in HR estimation. More sophisticated denoising techniques are thus required to obtain a clean heart sound signal under motion. Discrete wavelet transform (DWT) is therefore used to remove artefacts from the audio to isolate heart sounds. Specifically, we filter out detail coefficients

from the DWT based on signal variance, thus removing the noise components with a high variance from the mean.

Though denoising can yield a relatively clean heart sound signal, the denoised signals are still interfered by the motion artefacts to some extent, due to the underlying complexity of the artefacts. Therefore, we propose a frequency spectrum searching algorithm to estimate the HR from the denoised signal to account for the remaining motion artefacts. We first compute the spectrum of the denoised audio signals. Instead of searching the peaks over the full frequency range, we only search the HR peaks in a small frequency range corresponding to the range of allowable human HRs and the HR in the previous window. This guarantees that peaks in HR-unrelated frequency ranges are not taken as HR and the HR is temporally dependent on previous ones.

However, this system has some limitations including error propagation due to temporal dependencies of the algorithm and a lack of robustness to changes in signal properties. It was also unable to reconstruct the uncorrupted audio, meaning that the data could not be used for metrics other than heart rate. As such, we acknowledge that a more sophisticated approach to solving the problem, specifically to addressing signal denoising, is required.

3.2 Overview of DL-Based Pipeline

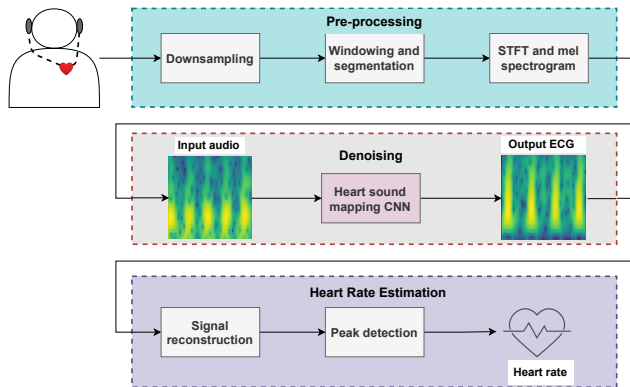


Figure 4: hEARt system flowchart.

An overview of hEARt, the designed motion-resilient HR monitoring system is given in Figure 4. Audio signals captured inside the occluded ear canal are used for HR estimation, which is performed in three stages: pre-processing, motion artefact (MA) elimination and HR estimation. Pre-processing aims at removing the unnecessary frequency components and converting the audio signals into a limited-bandwidth, matching the frequencies of interest of the heart sounds. For MA elimination, we proposed a CNN-based network to denoise the corrupted heart sounds by mapping them to the GT ECG signals during the training phase. Once trained, the CNN-based network can be directly employed to obtain clean heart sounds for HR estimation thus not requiring ECG for testing. Specifically, it maps the spectrogram of the heart sounds to the spectrogram of its corresponding ECG, a relatively clean version of the heart signal. We adopted a U-net encoder-decoder architecture for denoising [42]. Initially developed for biomedical image segmentation, U-net shows great potential in image super resolution

and image denoising [42, 49]. It captures the most important features in the audio spectrograms via an encoder, and reconstructs its corresponding clean heart signal via these salient representations via a decoder. Finally, HR is estimated using a peak estimation detection technique from the clean heart signals. More details can be found in the following sections.

3.3 Pre-processing

The heart sounds of interest captured by the in-ear microphone are low frequency signals with a bandwidth of less than 50 Hz. As such, to prepare the audio signals for processing, we first downsample the audio from 22 kHz to 1 kHz. We then segment the audio into 2 s windows, each with a 1.5 s overlap with the previous window. 2 s windows were selected as they ensure there will always be multiple heart beats (at least 2) within a window, thus allowing for inter-beat properties to be learned by the system. Each window is then band-pass filtered between 0.5 Hz and 50 Hz using a fourth order Infinite Impulse Response (IIR) Butterworth filter to remove any DC offset and high frequency signals. This attenuates the frequency components that are not of interest for HR calculation, including music and ambient noise. Additionally, due to occlusion of the ear canal, the majority of external noise is suppressed and not captured by the internally facing microphone. However, as outlined in Section 2.3, motion artefacts and other interfering signals lie overlapping frequency ranges with heart sounds, therefore, requiring additional processing.

We process the ground-truth similarly. The ECG, sampled at 130 Hz, is bandpass filtered between 10 and 50 Hz and then up-sampled to 1 kHz. The highpass cutoff for the ECG was selected to be 10 Hz as this was empirically found to emphasise the peaks in the ECG (the QRS complex) while attenuating the P wave and the T wave (as seen in Figure 2). Since we are only interested in capturing the beats and the inter-beat timing (for measuring HR, and in future, HRV), only the QRS complex is of interest in this work.

3.4 Motion Artefact Elimination

3.4.1 Spectrogram Generation. The motion artefact elimination subsystem takes as input the pre-processed audio signals, and outputs the cleaned heart signals. To do so, it uses the GT ECG signal to supervise the denoising of the heart signals. We compute the log-mel spectrograms for windowed audio and ECG signals using short-time Fourier transform (STFT), with a window size of 256 samples and a hop length of 32 samples. 1024 FFT bins are used with zero padding and Hann window is adopted. These parameters were selected as they visibly allowed for heart beats to be seen in the spectrograms. Thereafter, the log-mel spectrogram is computed using 64 mel bins. Log-mel spectrogram was chosen over spectrogram since it provides more detailed information in low frequency region, where heart sounds frequencies reside. The resulting log-mel spectrogram is a 64x64 matrix for each window. Since the audio is captured in both ears, a spectrogram is computed for each channel and these are stacked together to form one 64x64x2 input. The output is a single channel ECG spectrogram. The spectrograms are normalised between 0 to 1, which benefits the network training. It should be noted that the normalisation is carried out for all the

spectrograms by dividing a constant value, instead of normalising each spectrogram with its maximum value. This aims to maintain the difference in the signal amplitude for different activities.

3.4.2 Network Structure. Figure 5 provides the architecture of the U-Net used for denoising. In the encoder (or contraction path), the model consists of repeated 3x3 convolutions (with a ReLU activation function), batch normalisation and max pooling blocks with a stride of 2 to downsample the data. After pooling, dropout is applied with a rate of 0.1 to avoid overfitting. Each time the data is downsampled, the number of feature maps is doubled to enable the network to learn complex structures in the data. In the decoder (expansion path), the data undergoes successive up-convolutions where the number of feature maps is halved at each step. After each up-convolution, the feature maps are merged with the corresponding feature map from the encoder and then undergo the convolution and batch normalisation layers as in the encoder. In the final layer, a 1x1 convolution is used to map the final feature maps into a single 64x64 output image.

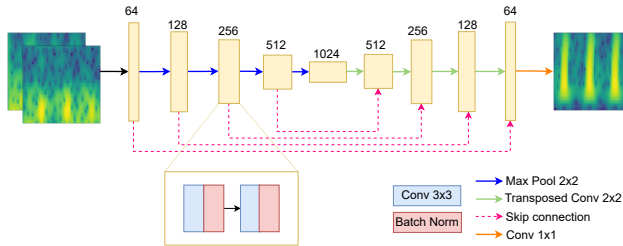


Figure 5: U-Net autoencoder architecture

3.4.3 Transfer Learning. On account of the small dataset, transfer learning is used to improve the results of the heart sound denoising. To achieve this, the model is pre-trained using the PASCAL heart sound database [8], where both the input and output to the network are log-mel spectrograms of heart sounds. By doing this, we aim to improve the ability of the network to extract representative audio features related to heart sounds. The pre-trained model weights are then set as the initialization weights for the CNN, which is further fine-tuned using our data. This helps leverage and transfer the knowledge learnt about heart sounds using PASCAL, as well as avoiding overfitting using small dataset.

3.4.4 Training. The input audio spectrograms and their corresponding ECG spectrograms are used to train the network. We use leave-one-out cross validation during training whereby each subject is held out as the test-set and a model trained on the other 19 users. The model is trained empirically for 100 epochs using the Adam optimizer with a learning rate of 0.001 and a batch size of 64. When choosing the training parameters, our objective was to strike a good balance between performance and computation complexity.

Mean square error (MSE) or L2 loss, as defined in Equation (1), is used as the loss function. This loss aims to minimise the distance between the GT ECG spectrogram (y_{ij}) and the noisy audio spectrogram (\hat{y}_{ij}), where i and j represents the time and frequency index respectively, and T and F represent the total number of bins over time and frequency dimension respectively.

$$MSE = \frac{1}{TF} \sum (y_{ij} - \hat{y}_{ij})^2 \quad (1)$$

3.4.5 Signal Reconstruction. We aim to convert the reconstructed clean spectrogram to time-domain waveforms for HR estimation. The Griffin-Lim algorithm is used for spectrum inversion. As each converted waveform is of 2 s duration and overlapped with 1.5 s, they are merged into a continuous time series signal by summing the overlapping regions.

3.5 Heart Rate Estimation

Heart rate estimation is performed in an 8 s long window, where each window has a 6 s overlap with the previous window. Each window undergoes the Hilbert transform to compute the envelope of the signal. Thereafter, a Gaussian moving average filter is applied to the envelope to smooth out small ripples and peaks in the signal. Finally, peak detection is calculated on the resultant signal, and the timings between consecutive peaks are used to compute the average heart rate for the window.

4 IMPLEMENTATION

In this section we present the implementation details of our system, describing our prototype as well as the methodology we followed to run our data collection campaign.

4.1 Prototyping

Although in-ear microphones have been integrated into existing commercial earbuds (e.g., AirPods Pro), no API is available to access the raw microphone output. In order to gather data and understand the potential of our approach, we developed our earbuds prototype by customizing the existing earbuds, as shown in Figure 6. Specifically, we embedded two analogue omnidirectional MEMS microphones (SPU1410LR5H-QB from Knowles) in a pair of wired earbuds (Dacomex Binaural Intra-Earphone), as shown in Figure 6a. The microphones were selected since they have a relatively flat frequency response from 10 Hz to 10 kHz, thus encompassing the frequency range of heart sounds, speech and motion artefacts. The microphones were then connected to a differential circuit for common mode rejection of power line noise and other system noise sources. The microphone signals are then sampled by an audio codec onto a Raspberry Pi 4B. We used the ReSpeaker Voice Accessory Hat as the audio codec. To make the system portable, the circuitry and Raspberry Pi were placed in a chest bag which was worn by the participants during the experiments as shown in Figure 6b. This ensured that the device did not interfere with the natural movement of the participants while undergoing the tasks.

Although the occlusion effect implies the possibility of detecting any bone-conducted sounds from the ear canal, measuring heart sounds with an in-ear microphone is extremely challenging. Unlike walking, which usually generates strong vibrations (peak amplitude can reach 1 as shown in Figure 3b), heart beat/movement is very subtle, resulting in a very weak heart sound. As shown in Figure 7a and Figure 7c, when using the earbud equipped with a silicon ear tip, it is difficult to identify heart beats from the in-ear microphone signal. We overcome this challenge by replacing the silicon ear tip with a foam ear tip, which (1) largely suppresses/absorbs the

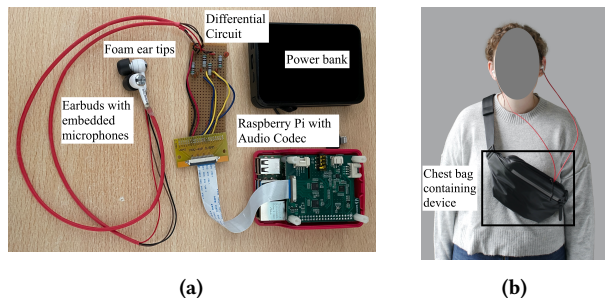


Figure 6: (a) Prototype and (b) participant wearing the device.

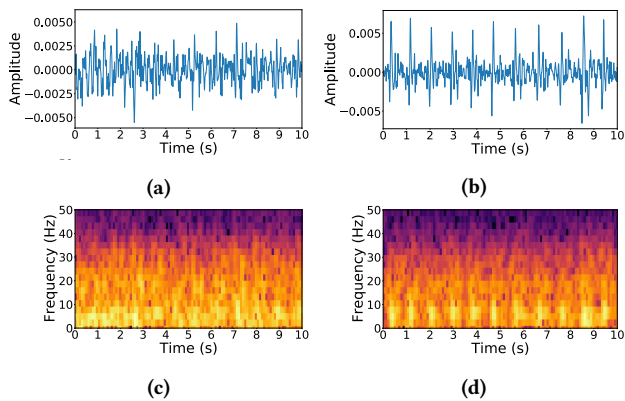


Figure 7: (a) Comparison of signals collected when the ear canal is occluded with a silicon ear tip ((a) and (c)) and with foam ear tip ((b) and (d)). The upper row plots the low pass filtered signal in the time domain, and the lower row plots its corresponding spectrogram.

external sounds, thereby resulting in a lower noise floor in the ear canal; (2) ensures a better sealing of the ear canal, thereby winning more amplification gain from the occlusion effect, as shown in Figure 7b and Figure 7d. With such upgrade, our prototype is able to measure heart sounds with a good signal-to-noise ratio (SNR).

4.2 Data Collection

We use an ECG chest strap (Polar H10) to measure the heart beat signal, which serves as the GT for HR. We extract the raw ECG from the Polar H10 and use it both as the clean ECG heart signal for the CNN and to calculate the GT heart rate. The microphone data was sampled at 22050 Hz and the ECG was sampled at 130 Hz. Due to the difference in two sampling frequencies, there is a maximum of a 150 ms delay between the audio and the ECG signal. However, since HR estimation is performed in 8 s windows, this delay is negligible in determining the HR. We synchronized the data by aligning the timestamps of the ECG signal with the timestamps of the recorded audio file.

Table 1: Heart rates recorded with the Polar H10 for the four activities.

Activity	Mean	Standard Deviation	Minimum	Maximum
Stationary	70	12	45	114
Walking	86	14	51	129
Running	109	23	50	167
Speaking	76	12	51	124

We invited 20 participants (13 males and 7 females) for data collection⁴. In addition to the stationary case, we considered three activities that are regarded as active or, that, because of their nature, interfere with the in-ear microphone: walking, running, and speaking. These activities were also selected as they match the conditions in [16] used to study in-ear PPG.

After wearing our earbud prototype and the ECG chest strap, the participants first kept stationary for 30 seconds to obtain the reference HR. Then, they performed each of the tasks continuously for 2 minutes. The 30 second stationary reference is only used for the baseline signal processing approach, and this data is not used in the hEART system. In designing our study protocol we favored shorter, but higher quality sessions over longer ones. It has been proven that longer data collection often yield lower quality data [13]. Bearing this in mind, the length of the sessions was carefully chosen to be long enough to yield good-quality vital signs and yet not too tedious to the participants.

When performing the walking and running activities, participants were allowed to pick a comfortable pace, and were instructed to move freely within a 5x4 m area. For the speaking activity, they were given a passage to read out loud.

We processed a total of 160 minutes of in-ear audio corresponding to the four tasks across all the participants. The data collection was done in the atrium of a busy building, and as such data was collected in the presence of uncontrolled ambient noise. This noise included human speech, the opening and closing of doors and low frequency power grid hum and air conditioning.

The data collected while running for participants 2 and 14 was excluded on account of poor data quality. This occurred because one of the earbuds fell out during the intensive running activity. This results in a lack of a proper seal between the ear and the earbud which means that the occlusion effect can not be leveraged.

The distribution of the GT HRs for each activity are provided in Table 1. From the table it is evident that the smallest variation in HR is found in the stationary cases, with the variation increasing as activity level increases. Likewise, the mean HR is highest for running and lowest when stationary.

5 PERFORMANCE EVALUATION

5.1 Metrics

We evaluated the performance of our system according to the following metrics [21]:

- Mean Absolute Error (MAE): the average absolute error between the GT HR (BPM_{true}) and the calculated HR (BPM_{calc})

⁴The experiment has been approved by the Ethics Committee of the institution.

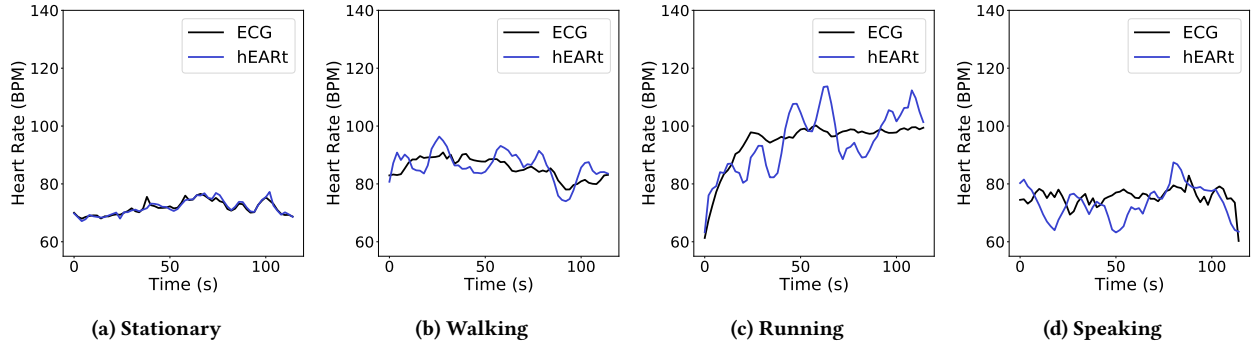


Figure 8: Qualitative longitudinal performance of heart rate extraction under different activities.

for each window $(i, i \in [1, N])$ as described in Equation (2).

$$MAE = \frac{1}{N} \sum_{i=1}^N |BPM_{calc}(i) - BPM_{true}(i)| \quad (2)$$

- Mean Average Percentage Error (MAPE): the average percentage error over each window (Equation (3)).

$$MAPE = \frac{1}{N} \sum_{i=1}^N \frac{|BPM_{calc}(i) - BPM_{true}(i)|}{BPM_{true}(i)} * 100 \quad (3)$$

- Modified Bland-Altman plots: a scatter plot indicating the difference between the two measurements (i.e. the bias or error) for every true value (i.e. HR from the GT). A modified Bland-Altman (BA) plot is constructed so that 95% of the data points lie within the limits of agreements of the two measurements (± 1.96 standard deviations of the mean difference between the methods) [17]. BA plots are used clinically to assess the level of agreement between two measurement methods [17]. In this work, we compare the calculated HR to the GT HR for each 8 s window.

5.2 Baseline Comparison

Table 2 shows the performance comparison between the proposed DL based hEART system and two signal processing approaches - (1) the proposed signal processing (SP) method (referred to as SP) leverages wavelet transforms for signal denoising and extracts HR from the frequency spectrum of the denoised signals. (2) we additionally compare our methods to the baseline developed by Martin and Voix [32] (referred to as baseline), which uses Hilbert transforms and peak detection for HR estimation in the time domain and under stationary conditions.

It is evident that the proposed SP approach outperforms the baseline significantly for stationary and running, and marginally for walking and talking, demonstrating that the baseline HR estimation algorithm designed for stationary is unable to effectively determine HR under motion and an additional denoising module is required. Thus, it is evident that the baseline approach is not able to generalize to motion conditions.

Comparing the SP with hEART, we observe that hEART does not outperform SP for stationary. This implies that signal processing techniques can be used whilst stationary and yield good HR estimation. However, with more intense motion interfering with the

heart sounds, SP fails to capture the HR from the signal and the performance severely deteriorates. hEART outperforms SP significantly with a relative improvement of 41%, 43% and 32% for walking, running and talking respectively, suggesting the effectiveness of hEART in HR estimation under motions.

The results for speaking are noticeably the worst of the four activities studied. This is consistent with Figure 3h, where it is clear that speaking brings more severe noises than the other activities. Perhaps against intuition, this is not on account of speech being detected by the microphone since the frequencies of *audible* human speech are significantly higher than those of interest in the hEART system. Rather, speaking causes movement of the jaw and head and deformation of the ear canal due to jaw movement. These movements result into low-frequency bone-conducted vibrations which could be interpreted as heart beats. They are also non-periodic and random in nature and are thus harder to remove, resulting in higher errors. This is in contrast to walking and running which are largely periodic and more homogeneous and thus easier to remove.

Table 2 provides a comparison of the performance of hEART with that of in-ear PPG (as studied by Ferlini et al [16]). It is evident from the table that although PPG is the gold-standard for wearable heart rate measurement, full-body motion causes significant degradation in the quality of HR measurement. We thus believe that in-ear audio could be used as an alternative to, or in combination with, in-ear PPG for HR measurement through the ear.

Table 2: Comparison between hEART, the two baselines and ITC PPG in terms of MAPE (%)

Activity	hEART	Signal Processing	Baseline [32]	ITC PPG [16]
Stationary	6.52 ± 8.67	4.93 ± 8.33	9.88 ± 6.93	—
Walking	11.47 ± 8.65	19.41 ± 16.03	20.90 ± 11.22	27.14
Running	12.17 ± 14.03	21.43 ± 15.30	34.28 ± 8.73	29.84
Speaking	15.94 ± 12.47	23.37 ± 9.39	24.23 ± 7.98	12.52

5.3 hEART Overall Performance

Figure 8 shows the qualitative assessment of hEART in tracking HR over time from in-ear audio. We compared the GT HR collected via ECG chest-strap with the one extracted from the in-ear audio for one participant over the four different activities. It can be observed

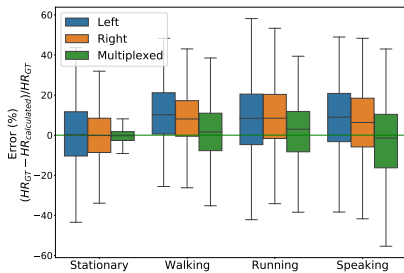


Figure 9: Sensor Multiplexing.

that the proposed approach is able to accurately and continuously track the user’s heart rate during the four activities (stationary, walking, running, and speaking), suggesting not only the potential of in-ear audio for HR estimation under MA, but also the effectiveness of the proposed pipeline. For speaking, the larger error is once again due to jaw movements. However, the overall trend of estimated HR still aligns with GT. Likewise in Figure 8c, there are periods of over and underestimation of the HR but it is evident that the trends of the two curves closely align. These spikes are due to the extremely low SNR of the heart sounds while undergoing intensive activity. Additional post-processing, which can be investigated in future, such as smoothing would further improve HR tracking and remove spikes in HR estimation.

Overall, the system achieves a MAE of 4.51 ± 6.01 BPM, 9.95 ± 7.62 BPM, 13.57 ± 10.51 BPM and 11.71 ± 8.59 BPM for stationary, walking, running and speaking respectively. As noted, we achieve the lowest performance during speaking in terms of MAPE as shown in Table 2. Concretely, given an average heart rate of 76 BPM (the mean HR while talking as per Table 1), a MAPE of 15.94% means our system misses (or adds) about 0.2 heart beats every second, or, 1 heart-beat every 5 seconds. Similarly, the performance achieved for running is even more convincing: at an average heart rate of 109 BPM (from Table 1) we miscompute 0.22 heart beats per second, again amounting to around 1 heart-beat every 5 seconds.

5.4 Sensor Multiplexing

In training the CNN, we use the signals from both earbuds. In this section, we evaluate the system performance using the signal recorded from each ear in isolation at test time. To do so, we stack the spectrogram created from the single ear on itself (thereby still creating a $64 \times 64 \times 2$ input to the trained model). This is an important use case of the system for the sake of energy efficiency and system complexity. Figure 9 shows how the median error varies between the left and the right earbud across the four activities. Additionally, for each of the four activities, the third value reported is the outcome of the fusion of the signal from the two earbuds (or using each ear as an input channel to the model). As expected, multiplexing the two signals yields better performance. The intuition behind this lays in the fact that both ears are experiencing the same phenomenon and this should give us a more robust signal. This is evident from the mean error which is reduced by multiplexing for all activities. Notably, we can also observe that in the stationary case, fusing the

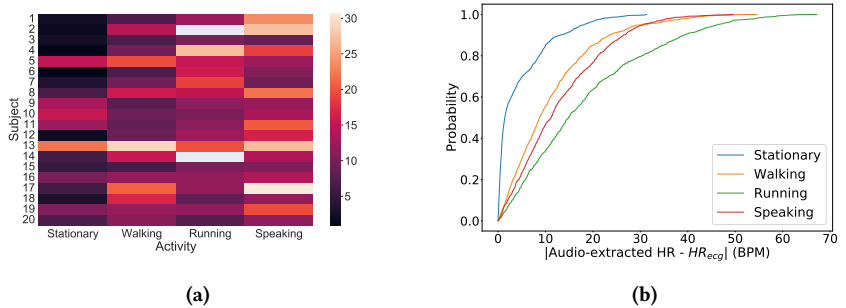


Figure 10: MAPE heatmap per subject (left) and empirical CDF plot (right).

signals substantially decreases the standard deviation. Likewise for walking and running, fusion significantly decreases the variance in the error. Interestingly, we also observe that although the mean error decreases, the standard deviation increases when multiplexing the signals from talking. This is perhaps due to the non-periodic and non symmetric nature of the motions involved in speech. When speaking, the jaw does not move identically on both sides [20], causing different noise artefacts in each ear. We believe that, unlike walking and running, these artefacts are different enough that fusing the signals hinders, rather than helps, performance.

5.5 Individual HR Estimation

Next, we evaluate our approach under different activities for all the subjects. First, we provide some insights on the population statistics. Figure 10a reports a heatmap showing the MAPE of the audio-extracted HR for every user across the four different activities. Lighter colors correspond to greater MAPE values. As expected, compared to the stationary baseline, the other three activities present greater errors for all users. The errors for running and walking are similar in magnitude. Interestingly, speaking is the activity that presents the greater variability and MAPE across subjects, as explained in Section 5.2. Overall, from Figure 10a, it can be observed how the technique generalizes well among all subjects, with some variability in higher motion activities: there are a few users from whom our approach performs poorly on a specific activity (e.g. user 1 and 4). For all users, this is likely due to an incorrectly fitting earbud in one ear which loosened during the activity, reducing the effect of the occlusion effect. Besides, as noted in Section 4.2, we had to remove running data from users 2 and 14 as the earable prototype fell out when performing the activity. The data that was removed is shown with white boxes (or NaN errors) in the heatmap. Additionally, there is one user for whom all of the results have a high error: user 13. This is again likely due to a poor fitting earbud, or to ground truth data of low quality. These issues would be solved by the use of wireless earbuds (ensuring that the wires do not dislodge the earbuds during activity) and by ensuring a higher quality earbud fit. Overall, these results prove that the system is able to generalize to different users and that with high quality data, good HR estimation can be achieved.

To further understand the extent to which the various activities impact our HR extraction technique, for each of them we report the empirical cumulative distribution function (ECDF) of the error (Figure 10b). Looking at the ECDFs we can confirm what was

observed in the heatmap. As expected, when the intensity of the motion increases, we observe greater errors. Specifically, our approach achieves an error of less than 15 BPM for over 60% of the users when the user is walking or speaking (low intensity motion artefacts). The errors ramp up to about 20 BPM for more than 60% of the study population whenever running is concerned. This performance on our academic prototype confirms that in-ear audio sensing of HR offers a promising alternative for continuous HR sensing in presence of motion.

5.6 Bland-Altman Plots

To further analyze the results, we leverage modified BA plots. We report the BA plots for the stationary case as well as for each of the motion artefacts in Figure 11. Specifically, Figure 11a reports the agreement between the HR calculated with hEARt and that obtained from the GT chest strap. By observing the plot, it is clear that the bias between the two measurements is minimal, with very low mean (only 0.54 BPM) and narrow limits of agreement (dashed red lines). Notably, the majority of the data points fall inside the limits of agreement, denoting the two measurements are in agreement. On the other hand, with more intense activities like walking and running (respectively in Figure 11b and Figure 11c), wider limits of agreement are present, representing a greater standard deviation in the HR estimation. Interestingly, while overall the mean errors remain low (-2.17 BPM for walking and -3.14 BPM for running), our approach exhibits a larger error for estimation when HR is above 100 BPM. We observed this phenomenon both for walking (Figure 11b) and running (Figure 11c) motions. Notably, especially in the running case, this is observed when the frequency of the running overlaps with the HR values. The spurious motion artefact-induced spikes trigger a harsher response by hEARt that tries to remove the noisy peaks, thus leading to an underestimation of the HR within 100 to 120 BPM. Additionally, another factor to explain the higher errors biased towards higher heart rates, could be traced back to the imbalance of our dataset, where lower HR values are predominant.

Finally, in Figure 11d, the mean error is the lowest of all the activities but with fairly wide limits of agreement. This wide standard deviation again points towards the complexity of the speaking activity, meaning that extrapolating useful heart signals to compute HR from in-ear audio signals is a very challenging task, never tackled before. Nonetheless, our approach still performs well.

5.7 In-the-wild performance

The results of the previous sections were obtained from experiments run under controlled conditions. To assess the real world effectiveness of the designed system, we collected an hour of data from one subject under conditions of daily life. During this time, the subject was instructed to undergo their activity as normal. This activity included working in an office, walking around, speaking (while working) and taking a short jog. The results of HR prediction for this study are provided in Figure 12. From the figure, it is evident that the tracker is able to accurately predict HR even in uncontrolled environments as the trends of the two lines match each other closely. However, as was seen in the BA plots in Section 5.6, the system underestimates the higher heart rates. This is likely

due to the distributions of heart rates in the dataset (as indicated in Table 1) where the average HR is 85 BPM. The average HR in the dataset is thus much lower than the maximum HR seen in the longitudinal study. This indicates that more training data at higher activities is needed for the network to generalize to all possible HRs. The underestimation could also be due to the filtering of the motion artefacts being too aggressive in the presence of higher frequency signals as these normally represent noise.

The MAE of this in-the-wild study is 7.39 BPM, which is a MAPE of 8.32%. To further break this down, the MAPE of activities A, B, C and D are 7.04%, 11.04%, 11.16%, and 8.32% respectively. If we compare these results to those in Table 2, we can see that all activities have comparable performance to that of the controlled experiments. The results of this study prove that the model is generalizable to different conditions and to different activities. It also shows that the model is able to make accurate predictions even under conditions of mixtures of activities. Thus this study acts as a proof of concept of the in-the-wild feasibility of the hEARt system.

5.8 Power and Latency Measurements

To provide a full system analysis, we also assess the power consumption and latency of the system implemented on the Raspberry Pi4. The trained hEARt CNN was converted to TensorFlow lite and deployed on the device. This mimics a stand-alone earable system whereby processing is done on device. Table 3 provides a breakdown of the operation times for the various components of the system. Signal denoising was performed on a 2 s window and HR extraction on an 8 s window, as detailed in Section 3.

Processing an eight-second window takes the system 54.35ms, implying that a new heart rate can be predicted by the system every 2s (due to the 6s second overlap between adjacent windows). This latency is an adjustable parameter of the system based on the overlap ratio.

The system power consumption is given in Table 4. Overall, the full system (including microphone sampling, denoising and HR prediction) consumes 701mW. The microphone sampling runs continuously, but the hEARt system is only active for 54.35ms for each HR estimate, and a HR estimate is made is every 2s. Thus, the average energy consumed per second is $(2871 - 2775)mW \times 1s + (3476 - 2871)mW \times 54.35ms/2 = 112.44mJ$. To place this in context, if run on a wireless earbud such as the Apple Airpod Pro (which has a battery capacity of 43mAh⁵), hEARt could operate continuously for a time $T = \frac{43mAh \times 5V}{115.26mJ} = 1.91hr$. While this may seem like a short operating time, this system has been implemented on a power hungry Raspberry Pi without optimizing for energy consumption. Additionally, when converting the denoising CNN to Tensorflow Lite, optimizations and quantization were not applied. As such the model used can further be optimized to reduce both energy consumption and latency. With such optimizations, the energy expenditure will be much lower. However, ultimately this gives an indication of how hEARt could feasibly be implemented on a commercial earbud.

⁵<https://www.ifixit.com/Teardown/AirPods+Pro+Teardown/127551>

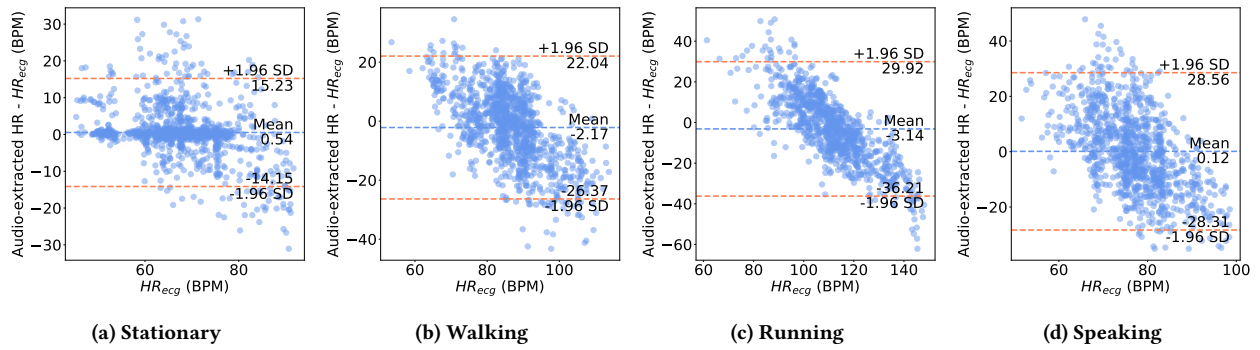


Figure 11: Modified Bland-Altman plot of heart rate extraction.

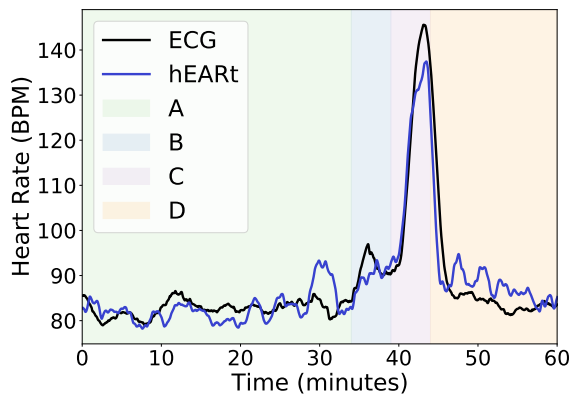


Figure 12: In-the-wild heart rate tracking. The coloured boxes indicate the different activities occurring during the study. A: Working while sitting. B: Walking. C: Running. D: Working while standing.

Table 3: Latency of hEARt

Operation	Latency (ms)
Preprocessing (per 2s window)	1.66
Denoising (per 2s window)	7.66
Signal reconstruction (per 8s window)	16.65
HR extraction (per 8s window)	0.42
Total (per 8s window)	54.35

Table 4: Power consumption of hEARt

Operation	Power (W)
RasPi (Baseline)	2.775
RasPi+Mic	2.871
Full system	3.476

6 DISCUSSION

Notably, while we acknowledge the merits of PPG-based heart rate monitoring and are aware of the wealth of information PPG carries, there is great value in showing the potential of a lesser explored

modality, such as in-ear microphones. As suggested by industrial research and market trends, it seems that ultra-miniaturized form factors will have a dominant role, especially as the distinction between hearing aids and earables is likely to become less marked. Additionally, in-ear facing microphones offer substantial advantages, starting from an overall price-tag. Besides, given their importance in noise cancellation in ANC (adaptive noise cancellation) earbuds, in-ear microphones have become a must-have feature for both high-end leisure earables and in hearing aids. Finally, microphones are relatively power efficient sensors [26], requiring far less current than, for instance, PPG (especially when used with high light intensity configurations to increase SNR) [34]. Concretely, the microphone we use [26] has a current draw of $0.12mA$, more than 10 times less than that of a state-of-the-art wearable dedicated PPG module [34]. In fact, even using the lower power configuration, the MAXM86161 optical module draws around $1.62mA$. Notably, if we were after higher PPG SNR, we would use their most performing configuration, which draws $3.78mA$.

In the remainder of this section we reason over some of the shortcomings of our work, and the potential solutions that we leave as future work. First and foremost, we are aware of the intrinsic limitations that comes with a simple, cheap prototype like ours. For instance, some of the collected data was corrupted as the subjects were unable to wear the earbuds properly, even though they were asked to fit them tightly. This indicates that the sealing of ear canal (i.e. the presence of the occlusion effect) is critical to our system. A couple of improvements could be introduced to address this issue. For example, given that people have different shaped and sized ear canals, it is necessary to select the optimal ear tip size for each individual. This might include an automated method of checking the fit of the earbuds and the seal as done by Ma et al. [31] or as that implemented by Apple for the AirPods Pro⁶. The data corruption during the running activities was also worsened by the wires on the earbuds which move during vigorous activity thus dislodging the earbuds for two of the participants. Using a wireless prototype would improve earbud fit and resulting system performance. However, as of today, manufactures still do not expose APIs for accessing in-ear audio. Interestingly, fit and positioning issues have been reported for in-ear photoplethysmography, too [16]. Though,

⁶<https://support.apple.com/en-us/HT210633>

contrary to PPG where sensor misplacement could be hard to identify and may lead to artefacts, poor fit is obvious in the case of in-ear microphones [31]. Nonetheless, our work shows the viability of using in-ear microphones for the detection of HR, even with a far-from-optimal prototype.

We note that the percentage errors in HR estimation while speaking require improvement to match the performance of PPG, although they are relatively comparable. Additionally, since the system aims to determine HR under active conditions (e.g., running), we expect the amount of speaking to be less than in non-active scenarios, limiting the impact of those errors especially over prolonged sequences. These errors occur since speaking introduces non-stationary noise that is different than walking and running, resulting in the activity not being as well processed using our current techniques. Other techniques to remove non-stationary noise can be considered. The quantity of non-stationary speaking samples could be increased during the training to make the model learn characteristics of these signals better.

Given the earbuds are mainly used for audio delivery, one concern is whether music playback will affect HR estimation performance. As studied by Ma et al. [31], in music, the average energy ratio below 50 Hz is only about 1.5%. This means that music has a negligible impact on our system as it operates on signals below 50 Hz. To confirm this, we first superimpose a music on the collected in-ear signals and filter it with a lowpass filter (pass band <50Hz). We then compute the Pearson correlation between the filtered signal and original in-ear signal, yielding a coefficient of 0.982, which further proves the robustness of our system.

Finally, despite the good performance, we expect more strategies to be utilized for further improvements. Firstly, we expect that fine tuning a model for each activity will improve activity level performance. We also aim to investigate the use of a LSTM-based model to better model dependencies between adjacent heart sounds. Additionally, collecting data from more subjects encompassing a wider range of heart rates will improve the ability of the model to further generalize to higher heart rates. An additional aspect left unexplored is whether personalization can help improve HR estimation. To achieve this, models could be fine-tuned using data from an individual user. Due to the differences in HRs and in heart sounds seen in the population, we expect that training the model using some of the user's own data would improve prediction accuracy. This would be particularly relevant for users with poor overall performance, as this indicates that the user's data is significantly different from that of the population. However, additional challenges to be solved around this involve the collection of this type of user data with reasonable labels.

7 RELATED WORK

7.1 Earables

Earables have attracted tremendous attention for human sensing applications, especially for health and well-being monitoring [24]. Extensive literature has investigated earables for blood flow and oxygen consumption [28], dietary monitoring and swallow detection [4, 29, 45], step counting [31], heart and respiratory rate tracking [32], user identification and gesture recognition [14], etc.

Bui et al. [11] proposed a device to measure blood pressure from the artery in the ear canal. Amft et al. [4] developed a monitoring system that classifies different kinds of food by analysing chewing sounds. With respect to motion tracking, facial expression tracking shows great potential, due to the physical deformations generated by facial muscle movements [33] [5]. An acoustic-based in-ear system using the in ear microphone for step counting, activity recognition, and hand-to-face gesture interaction was also investigated [31]. Respiratory rate measuring and biological analysis are also two vital application fields for earables [22, 41, 43].

A paradigm named HeadFi was proposed to turn the pair of drivers inside existing headphones into a sensor and validated its potential in four applications [14]. Using the HeadFi system, the authors perform HR monitoring in the stationary case and with the addition of body movement caused by taking the headphones on and off. However, they did not study HR monitoring in the presence of non-stationary, full-body motion such as running and walking, or speaking.

7.2 Heart rate monitoring

Heart rate is generally measured using electroencephalogram (EEG), ECG or PPG sensors. However, EEG has limited applications out-of-the-clinic and acquisition of ECG requiring wearing a chest belt makes it less convenient. Some smartwatches can capture ECGs, but require the user to close the circuit with their fingers. PPG is the gold-standard for HR monitoring in wearables. However, it is highly susceptible to motion artefacts caused by physical activity or motion of the user's body [21]. A recent study showed that amongst consumer and research grade wrist-worn wearables, the MAE of heart rate estimation was 30% higher during activity than at rest [7]. A particular problem with PPG is the signal crossover effect where the PPG sensors lock onto a periodic signal from motion (such as walking or running) and this motion is mistaken as the heart signal [7, 9, 37], causing measurement errors. Recently, [16] reported a 27.14%, 29.84% and 12.52% error of PPG sensors in earables for walking, running and speaking respectively, quantitatively demonstrating the challenges of PPG in HR estimation under motions.

Acoustic sensors have also been studied for heart rate measurements. Chen et al. [12] estimated heart rate from a small acoustic sensor placed at the neck, and [27] measured in-ear pulse wave velocity using heart signal as reference. A recent study examines both heart and breathing rates using microphones placed in the ear canal [32] mainly for stationary. Artefacts were found due to the subject's body movement even though all recordings are collected with test subjects seated in an audiometric double wall sound booth. [38] introduces a earphone that is equipped with an in-ear microphone to measure HR and an IMU to measure activity level. However, the impact of activity-induced vibrations on the in-ear heart sounds is not investigated. All these findings imply the challenges in heart rate measurement from earables under motion and we have presented an approach that aims to tackle these with the purpose of offering a solution to measuring HR in realistic settings.

8 CONCLUSION

We proposed an approach for accurate HR estimation using audio signals collected in the ear canal, under motion artefacts caused by daily activities (e.g., walking, running, and talking). Specifically, leveraging deep learning, we eliminate the interference of motion artefacts and recreate clean heart signals, from which we are able to determine HR. We designed a prototype and collected data from real subjects to evaluate the system. Experimental results demonstrate that our approach achieves mean absolute errors of 4.51 ± 6.01 BPM, 9.95 ± 7.62 BPM, 13.57 ± 10.51 BPM and 11.71 ± 8.59 BPM for stationary, walking, running and speaking, respectively, opening the door to new non-invasive and affordable HR monitoring with usable performance for daily activities. We also discussed some potential strategies to further improve the performance in the future.

REFERENCES

- [1] Jungmo Ahn, Ho-Kyeong Ra, Hee Jung Yoon, Sang Hyuk Son, and Jeonggil Ko. 2020. On-Device Filter Design for Self-Identifying Inaccurate Heart Rate Readings on Wrist-Worn PPG Sensors. *IEEE Access* 8 (2020), 184774–184784.
- [2] MA Ali and PM Shemi. 2015. An improved method of audio denoising based on wavelet transform. In *2015 international conference on Power, Instrumentation, Control and Computing (PICCC)*. IEEE, 1–6.
- [3] Mohammed Nabih Ali, EL-Sayed A El-Dahshan, and Ashraf H Yahia. 2017. Denoising of heart sound signals using discrete wavelet transform. *Circuits, Systems, and Signal Processing* 36, 11 (2017), 4482–4497.
- [4] Oliver Amft, Mathias Stäger, Paul Lukowicz, and Gerhard Tröster. 2005. Analysis of chewing sounds for dietary monitoring. In *International Conference on Ubiquitous Computing*. Springer, 56–72.
- [5] Toshiyuki Ando, Yuki Kubo, Buntarou Shizuki, and Shin Takahashi. 2017. Canalsense: Face-related movement recognition system based on sensing air pressure in ear canals. In *Proceedings of the 30th Annual ACM Symposium on User Interface Software and Technology*. 679–689.
- [6] Abdelkareem Bedri, David Byrd, Peter Presti, Himanshu Sahni, Zehua Gue, and Thad Starner. 2015. Stick it in your ear: Building an in-ear jaw movement sensor. In *Adjunct Proceedings of the 2015 ACM International Joint Conference on Pervasive and Ubiquitous Computing and Proceedings of the 2015 ACM International Symposium on Wearable Computers*. 1333–1338.
- [7] Brinnae Bent, Benjamin A Goldstein, Warren A Kibbe, and Jessilyn P Dunn. 2020. Investigating sources of inaccuracy in wearable optical heart rate sensors. *npi Digital Medicine* 3, 1 (12 2020), 18. <https://doi.org/10.1038/s41746-020-0226-6>
- [8] P. Bentley, G. Nordehn, M. Coimbra, and S. Mannor. [n.d.]. The PASCAL Classifying Heart Sounds Challenge 2011 (CHSC2011) Results. <http://www.peterjbentley.com/heartchallenge/index.html>.
- [9] Dwaipayan Biswas, Neide Simões-Capela, Chris Van Hoof, and Nick Van Helleputte. 2019. Heart rate estimation from wrist-worn photoplethysmography: A review. *IEEE Sensors Journal* 19, 16 (2019), 6560–6570.
- [10] Mahdi Boloursaz Mashhadi, Ehsan Asadi, Mohsen Eskandari, Shahrzad Kiani, and Farokh Marvasti. 2016. Heart Rate Tracking Using Wrist-Type Photoplethysmographic (PPG) Signals during Physical Exercise with Simultaneous Accelerometry. *IEEE Signal Processing Letters* 23, 2 (Feb. 2016), 227–231. <https://doi.org/10.1109/LSP.2015.2509868>
- [11] Nam Bui, Nhat Pham, Jessica Jacqueline Barnitz, Zhanan Zou, Phuc Nguyen, Hoang Truong, Taeho Kim, Nicholas Farrow, Anh Nguyen, Jianliang Xiao, Robin Deterding, Thang Dinh, and Tam Vu. 2019. eBP: A Wearable System For Frequent and Comfortable Blood Pressure Monitoring From User’s Ear. In *The 25th Annual International Conference on Mobile Computing and Networking (MobiCom ’19)*. Association for Computing Machinery, New York, NY, USA, 1–17. <https://doi.org/10.1145/3300061.3345454>
- [12] Guangwei Chen, Syed Anas Imtiaz, Eduardo Aguilar-Pelaez, and Esther Rodriguez-Villegas. 2015. Algorithm for heart rate extraction in a novel wearable acoustic sensor. *Healthcare technology letters* 2, 1 (2015), 28–33.
- [13] Wenqiang Chen, Shupai Lin, Elizabeth Thompson, and John Stankovic. 2021. SenseCollect: We Need Efficient Ways to Collect On-body Sensor-based Human Activity Data! *Proceedings of the ACM on Interactive, Mobile, Wearable and Ubiquitous Technologies* 5, 3 (2021), 1–27.
- [14] Xiaoran Fan, Longfei Shangguan, Siddharth Rupavatharam, Yanyong Zhang, Jie Xiong, Yunfei Ma, and Richard Howard. 2021. HeadFi: bringing intelligence to all headphones. In *Proceedings of the 27th Annual International Conference on Mobile Computing and Networking*. 147–159.
- [15] Andrea Ferlini, Dong Ma, Robert Harle, and Cecilia Mascolo. 2021. EarGate: gait-based user identification with in-ear microphones. In *Proceedings of the 27th Annual International Conference on Mobile Computing and Networking*. 337–349.
- [16] Andrea Ferlini, Alessandro Montanari, Chulhong Min, Hongwei Li, Ugo Sassi, and Fahim Kawsar. 2021. In-Ear PPG for Vital Signs. *IEEE Pervasive Computing* (2021).
- [17] Davide Giavarina. 2015. Understanding Bland Altman analysis. *Biochemia Medica* 25, 2 (2015), 141–151. <https://doi.org/10.11613/BM.2015.015>
- [18] Lovedeep Gondara. 2016. Medical image denoising using convolutional denoising autoencoders. In *2016 IEEE 16th international conference on data mining workshops (ICDMW)*. IEEE, 241–246.
- [19] Valentin Goverdovsky, Wilhelm Von Rosenberg, Takashi Nakamura, David Looney, David J Sharp, Christos Papavassiliou, Mary J Morrell, and Danilo P Mandic. 2017. Hearables: Multimodal physiological in-ear sensing. *Scientific reports* 7, 1 (2017), 1–10.
- [20] Roger Graves, Harold Goodglass, and Theodor Landis. 1982. Mouth Asymmetry during Spontaneous Speech. *Neuropsychologia* 20, 4 (1982), 371–381. [https://doi.org/10.1016/0028-3932\(82\)90037-9](https://doi.org/10.1016/0028-3932(82)90037-9)
- [21] Shahid Ismail, Usman Akram, and Imran Siddiqi. 2021. Heart rate tracking in photoplethysmography signals affected by motion artifacts: a review. , 5 pages. <https://doi.org/10.1186/s13634-020-00714-2>
- [22] Kamal Jafarian, Kamran Hassani, D. John Doyle, Mohammad Niakan Lahiji, Omid Moradi Moghaddam, Ala Saket, Mahsa Majidi, and Farhad Izadi. 2018. Color spectrographic respiratory monitoring from the external ear canal. *Clinical Science* 132, 24 (Dec. 2018), 2599–2607. <https://doi.org/10.1042/CS20180748>
- [23] Greeshma Joseph, Almaria Joseph, Geevarghese Titus, Rintu Mariya Thomas, and Dency Jose. 2014. Photoplethysmogram (PPG) Signal Analysis and Wavelet de-Noiseing. In *2014 Annual International Conference on Emerging Research Areas: Magnetics, Machines and Drives (AICERA/iCMMD)*. 1–5. <https://doi.org/10.1109/AICERA.2014.6908199>
- [24] Fahim Kawsar, Chulhong Min, Akhil Mathur, and Allesandro Montanari. 2018. Earables for Personal-Scale Behavior Analytics. *IEEE Pervasive Computing* 17, 3 (July 2018), 83–89. <https://doi.org/10.1109/MPRV.2018.03367740>
- [25] B.S. Kim and S.K. Yoo. 2006. Motion Artifact Reduction in Photoplethysmography Using Independent Component Analysis. *IEEE Transactions on Biomedical Engineering* 53, 3 (March 2006), 566–568. <https://doi.org/10.1109/TBME.2005.869784>
- [26] Knowles Electronics. 2013. *Zero-Height SiSonic Microphone With Extended Low Frequency Performance*. Knowles Electronics. Rev. D.
- [27] Roman Kusche, Paula Klimach, Ankit Malhotra, Steffen Kaufmann, and Martin Ryschka. 2015. An in-ear pulse wave velocity measurement system using heart sounds as time reference. *Current Directions in Biomedical Engineering* 1, 1 (2015), 366–370.
- [28] Steven F LeBoeuf, Michael E Aumer, William E Kraus, Johanna L Johnson, and Brian Duscha. 2014. Earbud-Based Sensor for the Assessment of Energy Expenditure, Heart Rate, and VO2max. *Medicine and science in sports and exercise* 46, 5 (5 2014), 1046–1052. <https://doi.org/10.1249/MSS.000000000000183>
- [29] Roya Lotfi, George Tzanetakis, Rasit Eskicicloglu, and Pourang Irani. 2020. A comparison between audio and IMU data to detect chewing events based on an earable device. In *Proceedings of the 11th Augmented Human International Conference*. ACM, Winnipeg Manitoba Canada, 1–8. <https://doi.org/10.1145/3396339.3396362>
- [30] Xugang Lu, Yu Tsao, Shigeki Matsuda, and Chiori Hori. 2013. Speech enhancement based on deep denoising autoencoder. In *Interspeech*, Vol. 2013. 436–440.
- [31] Dong Ma, Andrea Ferlini, and Cecilia Mascolo. 2021. OESense: Employing Occlusion Effect for in-Ear Human Sensing. In *Proceedings of the 19th Annual International Conference on Mobile Systems, Applications, and Services (Virtual Event, Wisconsin) (MobiSys ’21)*. Association for Computing Machinery, New York, NY, USA, 175–187. <https://doi.org/10.1145/3458864.3467680>
- [32] A Martin and J Voix. 2018. In-Ear Audio Wearable: Measurement of Heart and Breathing Rates for Health and Safety Monitoring. *IEEE Transactions on Biomedical Engineering* 65, 6 (2018), 1256–1263. <https://doi.org/10.1109/TBME.2017.2720463>
- [33] Denys JC Matthies, Bernhard A Strecker, and Bodo Urban. 2017. Earfieldsensing: A novel in-ear electric field sensing to enrich wearable gesture input through facial expressions. In *Proceedings of the 2017 CHI Conference on Human Factors in Computing Systems*. 1911–1922.
- [34] Maxim Integrated. 2019. *Single-Supply Integrated Optical Module for HR and SpO2 Measurement*. Maxim Integrated. Rev. 0.
- [35] Scott Michael, Kenneth S. Graham, and Glen M. Davis. 2017. Cardiac Autonomic Responses during Exercise and Post-exercise Recovery Using Heart Rate Variability and Systolic Time Intervals-A Review. *Frontiers in Physiology* 8 (2017), 301. <https://doi.org/10.3389/fphys.2017.00301>
- [36] MP Murray, GB Spurr, SB Sepic, GM Gardner, and LA Mollinger. 1985. Treadmill vs. floor walking: kinematics, electromyogram, and heart rate. *Journal of applied physiology* 59, 1 (1985), 87–91.
- [37] James W Navalta, Jeffrey Montes, Nathaniel G Bodell, Robert W Salatto, Jacob W Manning, and Mark DeBeliso. 2020. Concurrent heart rate validity of wearable technology devices during trail running. *Plos one* 15, 8 (2020), e0238569.

- [38] Shahriar Nirjon, Robert F Dickerson, Qiang Li, Philip Asare, John A Stankovic, Dezhi Hong, Ben Zhang, Xiaofan Jiang, Guobin Shen, and Feng Zhao. 2012. Musicalheart: A hearty way of listening to music. In *Proceedings of the 10th ACM Conference on Embedded Network Sensor Systems*. 43–56.
- [39] Stefanie Passler, Niklas Müller, and Veit Senner. 2019. In-ear pulse rate measurement: a valid alternative to heart rate derived from electrocardiography? *Sensors* 19, 17 (2019), 3641.
- [40] James AC Patterson, Douglas C McIlwraith, and Guang-Zhong Yang. 2009. A flexible, low noise reflective PPG sensor platform for ear-worn heart rate monitoring. In *2009 sixth international workshop on wearable and implantable body sensor networks*. IEEE, 286–291.
- [41] G.A. Pressler, J.P. Mansfield, H. Pasterkamp, and G.R. Wodicka. 2004. Detection of Respiratory Sounds at the External Ear. *IEEE Transactions on Biomedical Engineering* 51, 12 (Dec. 2004), 2089–2096. <https://doi.org/10.1109/TBME.2004.836525>
- [42] Olaf Ronneberger, Philipp Fischer, and Thomas Brox. 2015. U-Net: Convolutional Networks for Biomedical Image Segmentation. In *Medical Image Computing and Computer-Assisted Intervention – MICCAI 2015*, Nassir Navab, Joachim Hornegger, William M. Wells, and Alejandro F. Frangi (Eds.), Vol. 9351. Springer International Publishing, Cham, 234–241. https://doi.org/10.1007/978-3-319-24574-4_28
- [43] Tobias Röddiger, Daniel Wolfram, David Laubenstein, Matthias Budde, and Michael Beigl. 2019. Towards Respiration Rate Monitoring Using an In-Ear Headphone Inertial Measurement Unit. In *Proceedings of the 1st International Workshop on Earable Computing*. ACM, London United Kingdom, 48–53. <https://doi.org/10.1145/3345615.3361130>
- [44] Michael A. Stone, Anna M. Paul, Patrick Axon, and Brian C.J. Moore. 2014. A technique for estimating the occlusion effect for frequencies below 125 Hz. *Ear and Hearing* 35, 1 (1 2014), 49–55. <https://doi.org/10.1097/AUD.0b013e31829f2672>
- [45] Kazuhiro Taniguchi, Hisashi Kondo, Mami Kurosawa, and Atsushi Nishikawa. 2018. Earable TEMPO: A Novel, Hands-Free Input Device that Uses the Movement of the Tongue Measured with a Wearable Ear Sensor. *Sensors* 18, 3 (3 2018), 733. <https://doi.org/10.3390/s18030733>
- [46] Andriy Temko. 2017. Accurate Heart Rate Monitoring During Physical Exercises Using PPG. *IEEE Transactions on Biomedical Engineering* 64, 9 (Sept. 2017), 2016–2024. <https://doi.org/10.1109/TBME.2017.2676243>
- [47] Juergen Tonndorf. 1968. A new concept of bone conduction. *Archives of Otolaryngology* 87, 6 (1968), 595–600.
- [48] Karri Haen Whitmer. 2021. Assessment of Cardiovascular Function. *A Mixed Course-Based Research Approach to Human Physiology* (Feb. 2021).
- [49] Wenna Xu, Xinpeng Deng, Shanxin Guo, Jinsong Chen, Luyi Sun, Xiaorou Zheng, Yingfei Xiong, Yuan Shen, and Xiaoqin Wang. 2020. High-Resolution U-Net: Preserving Image Details for Cultivated Land Extraction. *Sensors (Basel, Switzerland)* 20, 15 (July 2020), 4064. <https://doi.org/10.3390/s20154064>
- [50] Yifan Zhang, Shuang Song, Rik Vullings, Dwaipayan Biswas, Neide Simões-Capela, Nick Van Helleputte, Chris Van Hoof, and Willemijn Groenendaal. 2019. Motion artifact reduction for wrist-worn photoplethysmograph sensors based on different wavelengths. *Sensors* 19, 3 (2019), 673.